J. Fluid Mech. (2006), *vol.* 548, *pp.* 49–68.
doi:10.1017/S0022112005007421 Printed in the United Kingdom

On gravity currents in a linearly stratified ambient: a generalization of Benjamin's steady-state propagation results

By M. UNGARISH

Department of Computer Science, Technion, Haifa 32000, Israel

(Received 21 January 2005 and in revised form 21 July 2005)

This paper presents a generalization of the classical results of T. B. Benjamin (*J. Fluid. Mech.* vol. 31, 1968, p. 209) concerning the propagation of a steady gravity current into a homogeneous ambient, to the case of a stratified ambient. The current of thickness h and density ρ_c propagates, with speed U, at the bottom of a long horizontal channel of height H, into the unperturbed ambient whose density increases linearly from ρ_o (at the top) to ρ_b (at the bottom). The reduced gravity is $g' = (\rho_c/\rho_o - 1)g$ and the governing parameters are $a = h/H$ and $S = (\rho_b - \rho_o)/(\rho_c - \rho_o)$, with $0 < a < 1, 0 < S < 1$; here g is the acceleration due to gravity. For a Boussinesq high-Reynolds two-dimensional configuration, a flow-field solution of Long's model, combined with flow-force balance over the width of the channel, are used for obtaining the desired results, in particular: $Fr = U/(g'h)^{1/2}$, head loss (dissipation), and criticality of U with respect to the fastest internal wave mode. The classical results of Benjamin are fully recovered for $S \to 0$. For small S and fixed a, the values of Fr and head loss are shown to decrease with S like $(1-2S/3)^{1/2}$ and $(1-2S/3)$, respectively, and the propagation is supercritical. For larger S several solutions are possible (for a given geometry a), mostly in the subcritical regime. Considerations for the physical acceptability of the multiple results are presented, and the connection with observations from lock-release experiments are discussed. The conclusion is that the present results provide a reliable and versatile generalization of the classical unstratified problem.

1. Introduction

Benjamin's (1968) theory on the steady-state propagation of a gravity current into a homogeneous ambient is well known and almost automatically cited in all subsequent works on gravity currents. The prototype geometry is a long horizontal channel of height H filled with stationary ambient fluid of density ρ_o. Into this fluid, at the bottom of the channel, a layer (current) of denser fluid of density ρ_c and thickness h propagates with uniform velocity U. The driving force is the reduced gravity

$$g' = \epsilon\, g, \tag{1.1}$$

where g is the acceleration due to gravity and

$$\epsilon = \frac{\rho_c - \rho_o}{\rho_o}. \tag{1.2}$$

Another important dimensionless parameter is the fractional depth

$$a = h/H. \tag{1.3}$$

The natural scaling velocity is $(g'h)^{1/2}$. The pertinent scaled velocity of propagation, referred to as the Froude number of the current, is

$$\hat{U} = Fr = \frac{U}{(g'h)^{1/2}}. \tag{1.4}$$

Benjamin derived rigorously an explicit formula for the Froude number as a function of a, namely

$$Fr_B(a) = \left[\frac{(2-a)(1-a)}{1+a}\right]^{1/2} \tag{1.5}$$

(the subscript B is used to denote the classic Benjamin results).

Moreover, Benjamin proved that head loss occurs, in general, in the steady-state gravity current configuration. He showed that along each streamline in the ambient, the pressure drop below the ideal energy-conserving Bernoulli result, scaled with $\rho_o g'$, is given by

$$\Delta_B = h\,\frac{a(1-2a)}{2(1-a^2)} \tag{1.6}$$

(this result is independent of the height of the streamline). Consequently, the ideal energy-conserving case is restricted to $a = 0.5$ only, and the steady state is physically possible only for a current which occupies a fractional depth $a \leqslant a_{max} = 0.5$ (for a larger a the dissipation would be negative).

The key role played by this theory in the investigation of non-stratified problems provides strong academic and practical motivations for the development of the counterpart theory for the linearly stratified ambient. Indeed, the stratification of the ambient is a natural ingredient in practical gravity current systems. However, this problem has defied solution for four decades. No such theory, or at least a systematic extension to mild stratification effects, has been published, to the best of our knowledge. Some *ad hoc Fr* approximations for intrusions into a linearly stratified ambient were used by Kao (1976) and Manins (1976). Ungarish & Huppert (2002), on the basis of localized pressure-head consideration, developed a practical stratification adjustment factor to the non-stratified *Fr*. This formula was used as an essential ingredient of a predictive shallow-water (SW) model. The SW results agree well with experiments and numerical Navier–Stokes solutions (in particular of Maxworthy *et al.* 2002) in a wide range of S and a. This indicates that the suggested formula captures the main features well (at least in the lock-release context). However, this formula lacks a rigorous theoretical backing. More details will be presented in § 3.5.

This work attempts to present the linear stratified ambient counterpart of Benjamin's Froude-formula results. The configuration is sketched in figure 1. The density of the unperturbed ambient, on the right-hand side, increases linearly from ρ_o at the top to ρ_b at the bottom; the density of the current is, again, ρ_c (we consider $\rho_c \geqslant \rho_b$ cases). A new dimensional parameter enters the formulation, the relative magnitude of the stratification

$$S = \frac{\rho_b - \rho_o}{\rho_c - \rho_o}, \tag{1.7}$$

with $0 < S < 1$. Now *Fr* is a function of both a and S. We expect that the classical case is recovered in the limit of a very mild stratification, $S \to 0$. We assume an almost inviscid Boussinesq fluid (i.e. $Re = Uh/\nu \gg 1$ and $\epsilon \ll 1$, where ν is the kinematic viscosity of the fluid) and a shallow configuration in the sense that the typical horizontal length is large compared with h.

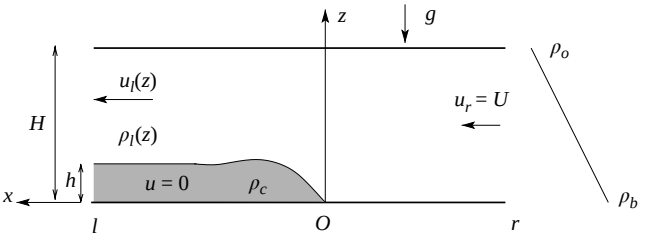

FIGURE 1. Sketch of the configuration. The lower boundary of the ambient is $z = \chi(x)$. r and l denote the upstream (right-hand) and the downstream (left-hand) positions.

The idea is to explore the similarity between the flow configuration used by Benjamin and a result of Long's model (Long 1953, 1955; Baines 1995) concerning the flow of a stratified fluid in a channel with an upper horizontal solid wall and a prescribed bottom topography. We use a frame of reference attached to the gravity current. As in Benjamin's case, the far upstream velocity of the ambient is constant over the height of the channel, $0 \leqslant z \leqslant H$. This flow climbs the topography (current) at a relatively slow pace (compared with the horizontal propagation). The streamlines become horizontal again in the far downstream region of the thinner channel, $h \leqslant z \leqslant H$. For an observer moving with the current (the bottom topography), the flow is steady. Total force, stability and dissipation considerations are applied to determine the velocity of a physically valid steady flow – in other words, the acceptable values of $\hat{U} = Fr$ for a given geometry and stratification. In Benjamin's case, the analysis is facilitated by the fact that the downstream flow of the ambient fluid regains a uniform velocity, $UH/(H-h)$. However, in the present case, owing to the linear density stratification in the upstream region, the horizontal downstream flow field of the ambient fluid develops a complex z-dependent structure of both the velocity and density. This difference introduces, besides quantitative changes in Fr, novel qualitative features.

The organization of the paper is as follows. In § 2, we formulate the flow field and derive the governing flow-force balance equation. In § 3, we present and analyse the results, in particular concerning the values of Fr and dissipation. Special attention is focused on the small S limit, i.e. small deviations from the classical Benjamin configuration. Comparisons with the experimental–numerical results of Maxworthy *et al.* (2002) and with previously suggested Fr formulae are also discussed. In § 4, some concluding remarks are given.

2. Formulation

2.1. *Steady-state flow pattern*

We start our analysis with a solution of a two-dimensional stratified flow field over a rigid bottom topography in a channel with an upper horizontal rigid lid at $z = H$, see figure 1. The horizontal and vertical coordinates are $\{x, z\}$, and the corresponding velocity components are $\{u, w\}$. Gravity acts in the $-z$-direction. To be specific, the obstacle (or topography) encountered by the unperturbed stratified fluid is defined by the bottom elevation function, $z = \chi(x)$. The value of χ is 0 (i.e. no obstacle) for non-positive x. For $x > 0$, the wall is elevated to $\chi(x) > 0$, and far downstream at the left-hand side, a parallel geometry is achieved again with $\chi(x) = h = \text{const} > 0$.

The far upstream flow (at the right-hand side, $x \to -\infty$), where the bottom is flat, $z = \chi(x) = 0$, consists of parallel horizontal streamlines with constant velocity U and

a prescribed stable linearly changing density. Using the subscript r (right) to denote this region, and employing the hydrostatic balance, we write

$$\left.\begin{aligned} &u_r(z) = U; \quad w_r(z) = 0; \quad \rho_r(z) = \rho_b - (\rho_b - \rho_o)\frac{z}{H}; \\ &p_r(z) = -g\int_0^z \rho_r(z')\,\mathrm{d}z' \quad (0 \leqslant z \leqslant H), \end{aligned}\right\} \tag{2.1}$$

where p is the pressure.

Under the assumption of a two-dimensional steady Boussinesq, inviscid and hydrostatic flow, Long's model procedure can be applied to reduce the set of governing Navier–Stokes equations to a single partial-differential equation for the displacement of the streamline, $\delta(x, z)$, with proper boundary conditions, in particular, $\delta = 0$ in the upstream right-hand region, and $\delta = \chi(x)$ at the bottom. The exact solution for the present configuration is reported in Baines (1995, § 5.7.1). The flow field is conveniently expressed with the aid of the perturbation (about the upstream flow) stream function, $-\partial\psi/\partial z = u'$, $\partial\psi/\partial x = w$, where $u = U + u'$. The result reads

$$\psi(x, z) = U\chi(x)\frac{\sin[\beta(1 - z/H)]}{\sin[\beta(1 - \chi(x)/H)]} = U\delta(x, z) \tag{2.2}$$

and

$$\rho(x, z) = \rho_b + (\rho_b - \rho_o)\left[-\frac{z}{H} + \frac{\chi(x)}{H}\frac{\sin[\beta(1 - z/H)]}{\sin[\beta(1 - \chi(x)/H)]}\right], \tag{2.3}$$

where

$$\beta = \frac{[(\rho_b/\rho_o - 1)gH]^{1/2}}{U} = \frac{(Sg'H)^{1/2}}{U} = \frac{\mathcal{N}H}{U} \tag{2.4}$$

and $\mathcal{N} = [(\rho_b/\rho_o - 1)g/H]^{1/2} = (Sg'/H)^{1/2}$ is the buoyancy frequency.

We combine this result with the presumed steady-state bottom gravity current. We replace the solid bottom obstacle with a stationary fluid of density ρ_c in the domain $(x \geqslant 0, 0 \leqslant z \leqslant \chi(x))$. The $\{x, z\}$-system is now a frame of reference attached to the gravity current, and the origin O is the front stagnation point. Following the lines of Benjamin's analysis, it is assumed that the dissipation effects in the resulting two-fluid system are relatively small (as confirmed below in § 3.4) and hence the structure of the parallel horizontal far up- and down-stream flow regions of the ambient, given by (2.2)–(2.3), is preserved. In this system, the right-hand upstream flow, where $\chi(x) = 0$, is unchanged and given by (2.1). In the left-hand (subscript l) region, where $\chi(x) = h$, the parallel horizontal flow satisfies

$$u_l(z) = \begin{cases} 0 & (0 \leqslant z < h), \\ U\left\{1 + \dfrac{a}{1-a}\dfrac{\gamma}{\sin\gamma}\cos\left[\dfrac{\gamma}{1-a}(1 - z/H)\right]\right\} & (h \leqslant z \leqslant H), \end{cases} \tag{2.5}$$

$$\rho_l(z) = \begin{cases} \rho_c & (0 \leqslant z < h), \\ \rho_r(z) + (\rho_b - \rho_o)\dfrac{a}{\sin\gamma}\sin\left[\dfrac{\gamma}{1-a}(1 - z/H)\right] & (h \leqslant z \leqslant H), \end{cases} \tag{2.6}$$

$$\delta_l(z) = \frac{h}{\sin\gamma}\sin\left[\frac{\gamma}{1-a}(1 - z/H)\right] \quad (h \leqslant z \leqslant H), \tag{2.7}$$

and, since $w_l = 0$, the hydrostatic balance yields

$$p_l(z) = p_O - g\int_0^z \rho_l(z')\,\mathrm{d}z' \tag{2.8}$$

where

$$\gamma = (1-a)\beta = (1-a)\sqrt{\frac{S}{a}}\frac{1}{\hat{U}} \tag{2.9}$$

and p_O is the pressure at the stagnation point O.

In the two-fluid flow field an equilibrium (steady state) can be maintained only for certain values of U. Following Benjamin, we consider the momentum balance in a fixed rectangular control volume whose lower and upper boundaries are the zero-stress planes $z = 0, H$, and the vertical boundaries are in the parallel up- and down-stream regions. The assumptions of steady-state and vanishing viscous stress (on the boundaries and in the horizontal flow domains) impose the flow-force balance

$$\int_0^H \left(\rho_l u_l^2 + p_l\right)\mathrm{d}z = \int_0^H \left(\rho_r u_r^2 + p_r\right)\mathrm{d}z. \tag{2.10}$$

At the stagnation point O, the pressure is $p_O = \rho_b U^2/2$ (recall that $p_r(z=0) = 0$). Using (2.1), (2.8) and (2.6), we obtain manageable expressions for the pressure terms in (2.10). The evaluation of the integral of the momentum flux terms in (2.10) is simplified by the Boussinesq assumption (i.e. $\rho_{l,r}(z)u_{l,r}^2(z) \approx \rho_o u_{l,r}^2(z)$; $u_{l,r}(z)$ are defined by (2.1) and (2.5)). After some tedious algebra and more use of the Boussinesq assumption, we can express the flow-force (2.10) balance as

$$\frac{\hat{U}^2}{2}\frac{1}{1-a}[1 + a - 2a^2 + a^2(\gamma^2 + (\gamma\cot\gamma)^2 + \gamma\cot\gamma)]$$
$$= 1 - \tfrac{1}{2}a + S\left[-1 + a - \tfrac{1}{3}a^2 + (1-a)^2\frac{1-\gamma\cot\gamma}{\gamma^2}\right]. \tag{2.11}$$

The right-hand side of (2.11) can be regarded as the buoyancy pressure driving, and the left-hand side as the dynamic reaction. The term multiplied by S is the contribution of the stratification to the (integrated) pressure difference. The last term in the brackets on the right-hand side is worth mentioning: it represents the effect of the displacement of the isopycnals.

Finally, we use (2.9) to eliminate $\hat{U}$ from (2.11) and obtain, after some algebra, the flow-force balance in the form

$$f(\gamma) = 1 - a + a(2-a)\gamma\cot\gamma + (a\gamma\cot\gamma)^2 + \gamma^2\frac{a}{1-a}\left[(2-a)\left(1-\frac{1}{S}\right) - \tfrac{1}{3}a^2\right] = 0. \tag{2.12}$$

The root(s) of this equation, for given a and S, provide the desired solution $Fr(a, S) = \hat{U} = (1-a)(S/a)^{1/2}/\gamma$ (see (2.9)). Obviously, only real-valued positive roots of $f(\gamma)$ are of interest in the physical context of the gravity-current problem. The Boussinesq simplification introduces an $O(\epsilon)$ error in the Fr results. We note that the stratification enters the relevant equation both explicitly as S and implicitly as (S/a) via γ. We could not find a rescaling which simplifies these dependencies (see § (3.3)). We think this reproduces a physical property of the system rather than a mathematical coincidence.

3. Results

3.1. *Small S (small γ)*

Consider the weak stratification, $S \to 0$, case. We expect that the dimensionless velocity $\hat{U} = Fr$ is of the order of unity. Note, however, that straightforward substitution of $S = \gamma = 0$ into (2.11) and (2.12) yields indeterminate 0/0 terms, and hence a more subtle calculation is required. Equation (2.9) indicates that $\gamma^2 = O(S)$. In this case, the use of (2.11) is convenient. By an expansion in powers of γ we obtain, to leading order in S, the compact result

$$\hat{U} = Fr(a, S) = \left[\frac{(2-a)(1-a)}{1+a}\left(1-\tfrac{2}{3}S\right)\right]^{1/2} = Fr_B(a)\left(1-\tfrac{2}{3}S\right)^{1/2} \tag{3.1}$$

where $Fr_B(a)$ is the classical formula of Benjamin, see (1.5). It is of course encouraging to find that the previous well-established result is a limiting case of the present theory. Moreover, it can be shown that the next term in the expansion will contribute in (3.1), following $2S/3$, a positive quantity of, approximately, $S^2/(90a)$. Thus, the approximation (3.1) is expected to be valid and fairly accurate for a wide range of S (say, $\leqslant 0.5$), provided that a is not very small, (say, $\geqslant 0.1$). This will be confirmed below by the numerical solution of $f(\gamma) = 0$. For $S < \epsilon$, the influence of S on Fr is within the Boussinesq error bounds. The resulting behaviour (3.1) is simple and intuitive: the weak stratification causes a mild reduction of Fr, which is effectively decoupled from the depth-ratio dependency.

The behaviour of a 'Froude number' of the current, which is actually a dimensionless velocity, depends, of course, on the scaling. This may become a confusing issue in the present stratified case where three densities and two lengths are present. We therefore recall our framework. It is convenient to consider the densities at the top of the ambient, ρ_o, and of the dense fluid, ρ_c, as given, with $\rho_c > \rho_o$. In most experimental settings, the top (open surface) is fresh water. The density in the ambient increases linearly with the depth. The bottom density, ρ_b, is between ρ_o and ρ_c, on a scale expressed by $0 < S < 1$. A weak stratification means that ρ_b is closer to ρ_o than to ρ_c. The scaling velocity in the present Fr is independent of ρ_b (or S). Thus, according to (3.1), for a given configuration, when a larger ρ_b is produced, the physical velocity of the current decreases. We think this is indeed simple and intuitive.

3.2. *Large γ. Validity-stability and criticality*

For non-small S and small a, the analysis is more complicated. It is necessary to find numerically the solution of (2.12). Now two difficulties appear.

First, an inspection of the equation indicates that, for non-small S, several simple positive roots may be obtained. We arrange the roots in increasing order, $\gamma_i, (i = 1, 2, \ldots)$. Secondly, we note that some roots may be larger than $\pi/2$. This introduces the possibility of negative u_l, as follows. Considering the contribution of the trigonometric term in (2.5), we find that (i) for $\gamma \leqslant \pi/2$, all values of $u_l(z)$ are positive and larger than U; but (ii) for certain values of $\gamma > \pi/2$ the velocity profile $u_l(z)$ above the current may attain negative values. This negative u_l situation invalidates the assumption that all the streamlines originate in the right unperturbed 'upstream' domain, and is unacceptable in the physical context of real gravity currents which propagate into the unperturbed ambient. Moreover, using (2.6), we find that $-\mathrm{d}\rho_l(z)/\mathrm{d}z$ has the same sign as $u_l(z)$. This means that the local stratification is unstable when u_l is negative. To quantify this tendency to negative velocity and instability in the downstream domain, we introduce the invalidity (or instability)

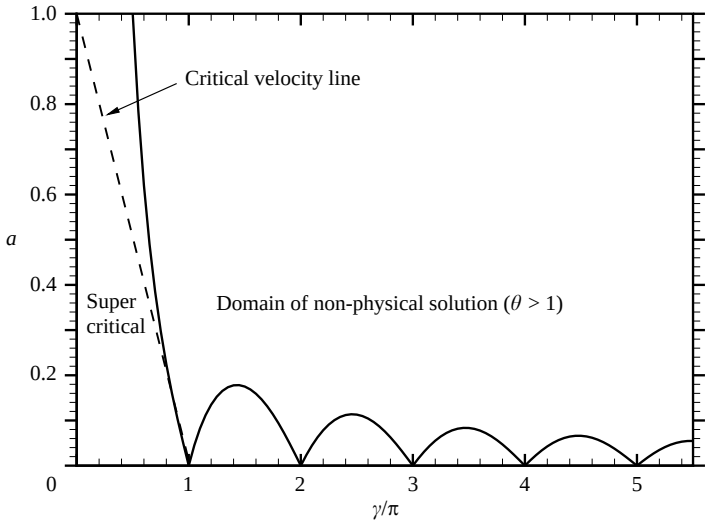

FIGURE 2. Domains of validity and criticality in the (γ, a)-plane. Points above and to the right-hand side of the solid line curve ($\theta = 1$) would produce negative and unstable downstream flows. Points on the left-hand side of the dashed critical velocity line correspond to supercritical currents; (on the right-hand side, to subcritical).

coefficient

$$\theta = \begin{cases} 0 & (0 < \gamma \leqslant \pi/2), \\ \dfrac{a}{1-a}\gamma|\cot\gamma| & (\pi/2 < \gamma < \pi), \\ \dfrac{a}{1-a}\dfrac{\gamma}{|\sin\gamma|} & (\pi < \gamma). \end{cases} \tag{3.2}$$

This is a measure of the most severe relative negative contribution of the perturbation flow to the resulting u_l. In other words, for $\gamma > \pi/2$, we obtain $\min(u_l) = U(1-\theta) < U$, and a tendency to unstable density variation, in at least one horizontal level. If θ is small, there is no danger of spurious behaviour, but for $\theta > 1$, the results are physically unacceptable. These unacceptable flow fields are also subject to shear instability (see Baines 1995), whereas, on the other hand, the criterion $\theta < 1$ is also sufficient for satisfying the $R_i > 0.25$ stability requirement in the ambient, where R_i is the Richardson number of the local flow.

In the following analysis, we are concerned only with 'valid' solutions, i.e. with roots of $f(\gamma) = 0$ which satisfy $\theta < 1$. Moreover, we monitor the values of θ in cases of non-unique valid roots; this is as a possible criterion for discrimination between the results (see below). The valid results are in the range $0 < \gamma \leqslant \max[\pi, (1-a)/a]$. A more detailed sketch of the validity domain in the (a, γ) plane is given in figure 2. For $a < 0.18$, a periodic validity pattern appears, and the number of these repetitions increases as a decreases. We found that the number of valid roots of (2.12) roughly follows this pattern. Decreasing a from 0.5 (see below § (3.4)), the first γ_2 (valid) solution was obtained for $a = 0.1784$ and $S = 0.875$; for larger values of a and $0 < S < 1$, only γ_1 solutions were found.

Typical valid results of Fr, obtained numerically from (2.12), are presented in figure 3 and 4. Figure 3 illustrates the very good accuracy of the approximation (3.1): for a given a, Fr starts with Benjamin's value at very small S, then decreases with S; the slope is very close to $-1/3$, independent of a. The deviation from this simple

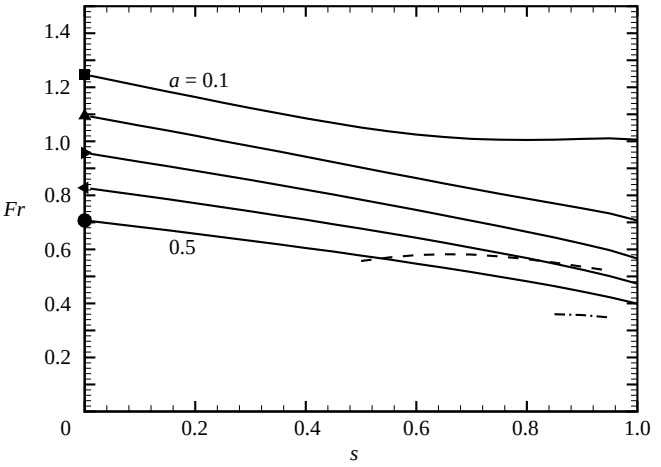

FIGURE 3. *Fr* as a function of *S* for $a = 0.1, 0.2, 0.3, 0.4, 0.5$. The symbols are Benjamin's solution for the corresponding *a*. The dashed and dash-dotted lines are the second and third roots for $a = 0.1$.

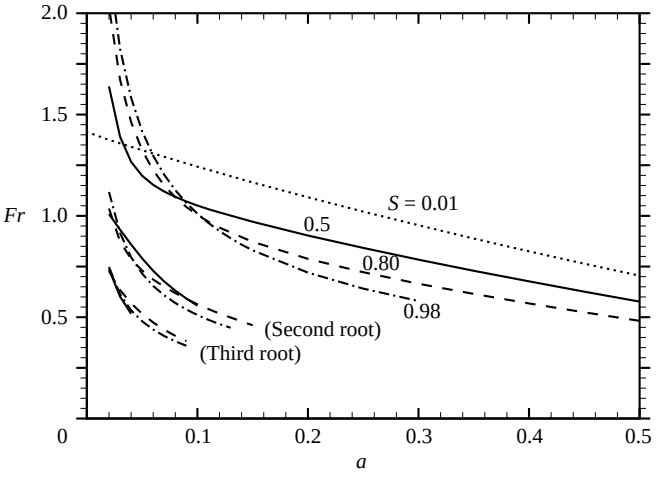

FIGURE 4. *Fr* as a function of *a* for various *S* ($S = 0.01$ dotted line, $S = 0.5$ solid line, $S = 0.8$ dashed line, $S = 0.98$ dash-dotted line).

behaviour appears for larger values of S/a (> 5, say). Here, a second-root branch may also appear.

The behaviour of the first-root solution seems bizarre (counter-intuitive) when S/a becomes large (> 5, say): for a fixed *a*, *Fr* reaches a minimum, then increases (slightly) with *S*. To understand this unexpected behaviour, we return to the flow-force balance (2.11), expand $\gamma \cot \gamma$ in powers of γ and truncate the results after the γ^4 term (the accuracy is within several per cent for $\gamma < 2.5$ and qualitatively sufficient for $\gamma < 3$). We obtain

$$\frac{\hat{U}^2}{2}\frac{1}{1-a}\left[(1+a)+\tfrac{2}{45}a^2\gamma^4\right] = \left(1-\tfrac{1}{2}a\right)\left(1-\tfrac{2}{3}S\right)+(1-a)^2\frac{S}{45}\left(\gamma^2+\tfrac{2}{21}\gamma^4\right). \quad (3.3)$$

The right-hand side is, again, the pressure force term, and the left-hand side the dynamic reaction. According to (2.9), $\gamma^2 \approx S/a$ in the range of interest here. The right-hand side pressure force displays the tendency to decrease the dimensionless speed $\hat{U}$ of the current when S increases from zero (the first term), but also the possibility of enhancing $\hat{U}$ when γ is not small (the last term). However, a simple analysis proves that the change of trend occurs at a large value of γ^2 (to be specific, the right-hand side reaches its minimum at $S/a \approx 7$). This can be achieved only for small values of a. A closer inspection shows that the enhancing component of the pressure term is a secondary contribution of the displacement of the isopycnals, i.e. the last term in (2.3). (The main contribution of the displacement is to reduce the coefficient of $-S$ in the first term of (3.3) from 1 to 2/3.) On the other hand, the effect of stratification on the left-hand side dynamic force term enters like $a^2\gamma^4$ and hence it remains bounded when a decreases. Actually, the relevant term is $0.05S^2$ approximately, for both small and non-small values of a. This change in the left-hand side term can be neglected as compared with the effect of the stratification on the right-hand side term. The behaviour of $\hat{U} = Fr$ discussed here is relevant for the first root only. When $\gamma \to \pi^-$ the results tend to violate the $\theta \leqslant 1$ restriction, see (3.2). When $\gamma > \pi$ the trigonometric terms change sign, the force balance admits a second (or higher) branch (root of $f(\gamma) = 0$). The branches of the additional roots, see figures 3 and 4, reproduce the expected decrease of Fr with increasing S. It is not clear if the counter-intuitive result is spurious, or may be realized under some complex initial/boundary conditions (e.g. a strong source). Our 'intuition' is mostly a result of simple lock-release tests, and under these conditions the subcritical second (or higher) branch solution is more likely to develop and prevail. We shall return to this point in § 3.5.

The velocity of the fastest internal gravity wave in the upstream section is (see Baines 1995),

$$U_w = \frac{\mathcal{N}H}{\pi} = \frac{(Sg'H)^{1/2}}{\pi}. \tag{3.4}$$

The ratio of U_w to the speed of the current can therefore be expressed as

$$\frac{U_w}{U} = \frac{\gamma}{\pi(1-a)} = \frac{1}{\pi}\sqrt{\frac{S}{a}}\frac{1}{Fr}. \tag{3.5}$$

The critical Fr number, for which this ratio is 1, is

$$Fr_{cr} = \frac{1}{\pi}\sqrt{\frac{S}{a}}. \tag{3.6}$$

The steady-state current under consideration is supercritical, i.e. propagates faster than U_w, if its $Fr > Fr_{cr}$ (i.e. $\gamma < \pi(1-a)$, see figure 2). This type of current is more likely to occur for configurations with small S and non-small a. The calculations show that valid results in the supercritical domain are obtained for, approximatively

$$S < \begin{cases} 0.9 + 0.25(0.5 - a) & (0.1 \leqslant a \leqslant 0.5), \\ 1 & (a < 0.1). \end{cases} \tag{3.7}$$

However, this apparent dominance of the supercritical regime is based on γ_1, the first valid root of $f(\gamma)$. The additional roots, when present, yield, without exception, subcritical propagation. We found that, for $a < 0.18$, subcritical currents are possible for approximately,

$$S > 0.03 + 4.58a. \tag{3.8}$$

For lock-release problems with small a and non-small S, the subcritical currents seem more physically acceptable (rather, expected) than the supercritical solution. The reasons are as follows. Since the flow develops from zero velocity conditions, it obviously encounters first the subcritical quasi-steady balance; if this is sufficiently stable, there is apparently no mechanism to accelerate the propagation further. This may explain why the theoretical $\mathrm{d}Fr/\mathrm{d}S > 0$ of the supercritical branch is inconsistent with available experimental observations. Moreover, the dissipation head loss in the subcritical flow is smaller, as shown in § 3.4.

3.3. *The effective g' and Fr rescaling*

In the foregoing analysis, we scaled the velocity with g' based on the density difference of the current to the top of the ambient, $\rho_c - \rho_o$. This scaling is convenient for homogeneous configurations and for presentation of laboratory results. Indeed, in typical experiments, the top of the ambient is fresh water, and it is straightforward to refer the other densities to this ρ_o. However, for enhancing the physical insights, in particular for non-small S, it makes sense to consider the results in a rescaled form. The choice of scaling parameters is, of course, non-unique. Moreover, owing to the complexity of the problem and the presence of oscillating trigonometric terms in the balances, a single scaling which is satisfactory for the full range of S and a is not expected. We shall briefly discuss one convenient approach.

We argue that the effective driving force of the current is well correlated to the difference between the density of the dense fluid, ρ_c, and the density of the upstream ambient at the mid-height of the head, $\rho_r(z = h/2)$. We therefore define the effective (subscript e) reduced gravity as

$$g'_e = \frac{\rho_c - \rho_r(h/2)}{\rho_o} g = \left(1 - S + \tfrac{1}{2}aS\right)g', \tag{3.9}$$

where (2.1), (1.1) and (1.7) were used. We note in passing that ρ_o was used as the denominator for simplicity; in the framework of the Boussinesq approximation, a negligible $O(\epsilon)$ change of g'_e appears if ρ_b or ρ_c is used instead. The scaling velocity is now $(g'_e h)^{1/2}$.

The effective Froude number is therefore defined as

$$Fr_e = \frac{U}{(g'_e h)^{1/2}} = \left(1 - S + \tfrac{1}{2}aS\right)^{-1/2} Fr, \tag{3.10}$$

see (1.4). The switch from the previous Fr results to the effective Froude is straightforward. Benjamin's scaling is fully recovered for $S \to 0$.

The rescaled Fr_e as a function of S for various values of a is displayed in figure 5 (to be compared with the counterpart figure 3 for the originally defined Fr). The conclusions are as follows.

Consider the weak stratification case, $S \leqslant 0.5$. The leading effect is contributed, again, by Benjamin's Fr_B. Indeed, the combination of (3.1) and (3.10) yields, to leading order in S

$$Fr_e = Fr_B(a)\left[1 + S\left(\tfrac{1}{3} - \tfrac{1}{2}a\right)\right]^{1/2}. \tag{3.11}$$

For $0.1 \leqslant a \leqslant 0.5$, the effective Froude number varies very little with S. This is because now the reference velocity takes into account the density stratification effect. In this case, our intuitive expectation of g'_e is confirmed. However, figure 5 shows that the counter-intuitive increase of Fr (for the first root) with S when S/a is not small has not been alleviated by this rescaling. On the contrary, this effect becomes more pronounced in the behaviour of the rescaled Fr_e. In other words, in this case

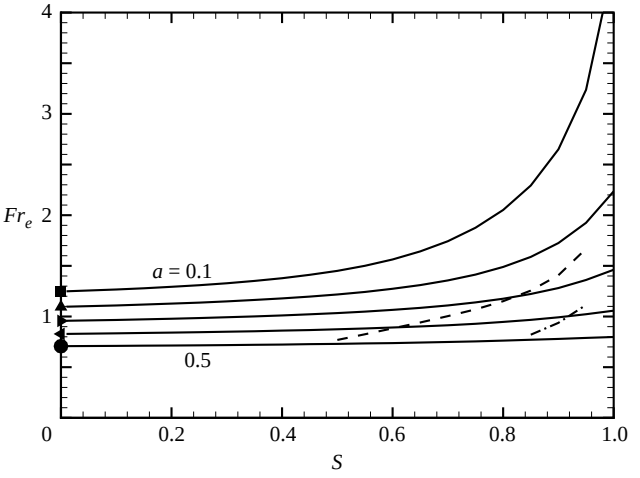

FIGURE 5. Fr_e as a function of S for $a = 0.1, 0.2, 0.3, 0.4, 0.5$. The symbols are Benjamin's solution for the corresponding a. The dashed and dash-dotted lines are the second and third roots for $a = 0.1$.

our intuitive understanding of g'_e is not sufficient for the interpretation of the flow; the real speed is significantly larger than expected. This strengthens our conclusion that this is a subtle physical effect, not a mathematical artefact. We conclude that the rescaling is helpful in the case of weak stratification, but may be misleading (significantly underestimate) the first root behaviour when $S/a > 5$.

Consider the strong stratification $S \to 1$ flow for small a, when the second (and third, etc.) root appears (the dashes and dashed-dotted lines in figure 5). Here, the advantage of the rescaling is observed: Fr_e is of the order of 1 (while the original Fr tends to small values). This turns out to fulfil our expectations. Indeed, the case $S \to 1$, i.e. $\rho_b \to \rho_c$, corresponds to an intrusion at the neutral-buoyancy level. In this case, we can write $g' = \mathscr{N}^2 H$, where, again, $\mathscr{N}$ is the buoyancy frequency. Our estimate of the velocity of propagation, based on physical intuition and supported by experimental and numerical evidence (Wu 1969; Amen & Maxworthy 1980; Ungarish 2005) is as follows. Since the density difference at $z = 0$ is zero, in this case the buoyancy driving effect is clearly provided by the gradient, g'/H, multiplied by the (half) thickness of the current. This produces the effective reduced gravity $g'_e = \mathscr{N}^2 h/2 = ag'/2$ (exactly as given by (3.9)). Consequently, the relevant expected speed of propagation is $(g'_e h)^{1/2} = (1/\sqrt{2})\mathscr{N} h$. The fact that Fr_e is of the order 1 indicates that there are stable solutions of the generalized Benjamin problem which agree well with our intuitive understanding of the flow field in this limit.

3.4. *Energy dissipation*

Consider a streamline at height z in the left-hand side parallel domain of ambient fluid. This streamline carries fluid of density $\rho_l(z)$ and is elevated $\delta_l(z)$ from the initial right-hand side position. In ideal conditions, the pressure on this streamline satisfies Bernoulli's equation

$$p_l^i(z) + \tfrac{1}{2}\rho_l(z)u_l^2(z) + \rho_l(z)\delta_l(z)g = p_r(z - \delta_l(z)) + \tfrac{1}{2}\rho_l(z)U^2 \quad (h \leqslant z \leqslant H), \qquad (3.12)$$

where the superscript i denotes ideal energy-conserving flow. For the non-ideal flow of the gravity current, following Benjamin, we introduce the head loss on the streamline

$$\Delta(z) = [p_l^i(z) - p_l(z)]/(\rho_o g') \quad (h \leqslant z \leqslant H). \tag{3.13}$$

In Benjamin's analysis the head loss is independent of z. For the present more complex configuration, it is convenient to define the average head loss

$$\overline{\Delta} = \frac{1}{H-h}\int_h^H \Delta(z)\,\mathrm{d}z. \tag{3.14}$$

Substituting (2.5)–(2.8) and (3.12) into (3.13) and using the fact that the density is preserved on the streamline we obtain, after some algebra,

$$\frac{\overline{\Delta}}{h} = 1 - S\left[1 - \tfrac{1}{2}a + \tfrac{1}{2}\frac{(1-a)^2}{a}\frac{1}{\gamma^2} + \tfrac{1}{2}a\frac{1}{\sin^2\gamma} + (1-a)\frac{\cot\gamma}{\gamma}\right]. \tag{3.15}$$

The results are meaningful for values of γ which are valid solutions of $f(\gamma)=0$.

For obtaining the behaviour for small S, we use an expansion of (3.15) in powers of γ combined with (2.9) and (3.1). This yields, to leading order in S, the compact result

$$\overline{\Delta} = h\,\frac{a(1-2a)}{2(1-a^2)}\left(1 - \tfrac{2}{3}S\right) = \Delta_B\left(1 - \tfrac{2}{3}S\right), \tag{3.16}$$

where Δ_B is the classical result, (1.6), for a non-stratified ambient. The fact that Benjamin's dissipation results are recovered for small values of S is, again, encouraging. In particular, it is evident that $\overline{\Delta}$ vanishes, to leading order, only for $a=0.5$, and becomes negative for larger a. This confirms, and also extends, the well-known outcome of Benjamin's analysis that in a homogeneous ambient only the half-depth current is energy conserving, and that for $a > 0.5$, the dissipation attains non-physical values. The last equation also indicates that the stratification reduces the dissipation.

In general, the numerical calculation of the dissipation via (3.15) in the domain of interest shows that for valid solutions of (2.12): (i) for a given a, $\overline{\Delta}/h$ decreases as S increases. This seems consistent with the observations of Maxworthy *et al.* (2002) that the interface of the current is smoother in the stratified ambient than in the homogeneous counterpart; (ii) For $a > 0.5$, only non-physical negative $\overline{\Delta}$ were obtained. Let $a_{max}(S)$ be the largest fractional depth for which physical non-negative dissipation occurs at a given S. Decreasing a from 1, we find that the largest a_{max} is 0.5 for small S, and becomes smaller than 0.5 as S increases. This is a generalization to $S > 0$ of Benjamin observation that in the homogeneous ambient the non-dissipative result is valid only for $a=0.5$, and that a steady flow is impossible in practice if the current occupies more than a certain portion of the channel (0.5 in his case).

Typical head-loss results are displayed in figure 6 and 7. In the tested cases, $0.05 \leqslant a \leqslant 0.5$, $0 < S < 1$, the value of $\overline{\Delta}/h$ is quite small, typically $2-5\,\%$. The maximum, attained for $S \approx 0$ and $a=0.25$, is 0.066. (Benjamin scaled $\overline{\Delta}$ with H which, we think, is less informative. In any case, for the variable $\overline{\Delta}/H = a(\overline{\Delta}/h)$ and $S \to 0$, we obtain the same maximum as Benjamin: 0.021 at $a=0.35$.) The second and third root solutions display very small dissipation, $\overline{\Delta}/h < 0.1\,\%$; the difference from an energy-conserving flow in this case is negligible.

3.5. *Comparisons*

No direct experimental data for $Fr(a, S)$ is available, to our knowledge. We hope that the present analysis, which provides the theoretical background and values for

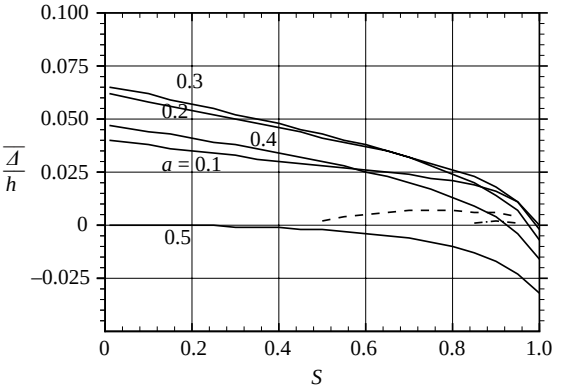

FIGURE 6. Head loss as a function of S for various a. The dashed and dash-dotted lines correspond to the second and third roots for $a = 0.1$.

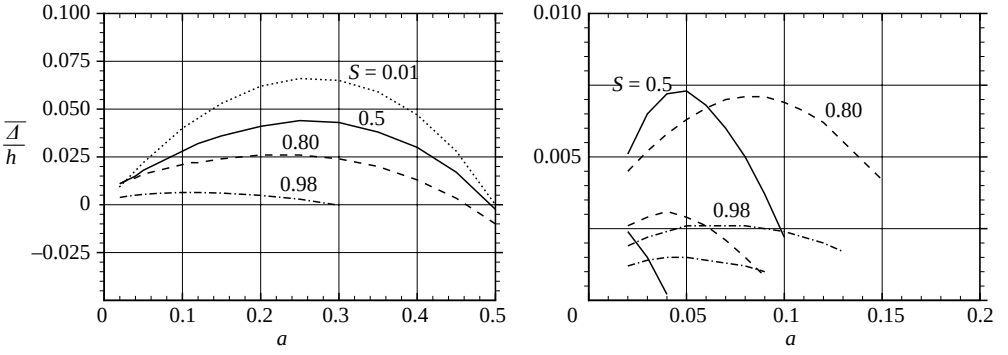

FIGURE 7. Head loss as a function of a for various S. (a) First root; (b) second and third roots.

comparisons, will motivate the appropriate experimental investigation. At present, the only closely related available experimental–numerical tests for a stratified ambient are by Maxworthy *et al.* (2002), to be discussed below. Even for the homogeneous ambient, the direct experimental verification of Benjamin's theory is a complex task. First, it is not easy to produce and control a steady-state gravity current which moves like a slug and whose stagnation point is at the bottom, see Simpson & Britter (1979). Secondly, it is not clear how to define the pertinent height h of a real current, because a thick mixed-fluid interface usually develops in practical circumstances. Attempts have been made (including by Benjamin) to infer the validity of the theoretical Fr from the measured velocity of propagation of the head in time-dependent currents, typically produced by release of a fixed volume of fluid from behind a lock. These efforts have been augmented by 'numerical experiments' (Klemp, Rotunno & Skamarock 1994, Härtel, Meiburg & Necker 2000). In a simple rectangular geometry the initial ('slumping') motion is with constant velocity, in accord with Benjamin's theory, but the shape of the interface changes with time (the dam-break problem) and hence the violation of the steady-state assumption cannot be fully dismissed. Comparisons of the theoretical predictions of the velocity with the measured values involve the Fr formula, but also a SW model, and hence the conclusions cannot be sharp. In general, the comparisons with experiments in homogeneous fluid show that Benjamin's Froude

formula gives the correct dependency on a, but overpredicts (by about 30 %) the value. The discrepancy is attributed mainly to viscous effects. Typical results are presented in Simpson & Britter (1979, figure 11), Hupper & Simpson (1980, figure 1), Klemp *et al.* (1994, figure 6*a*) and Härtel *et al.* (2000, figure 4.)

Shin, Dalziel & Linden (2004) challenged the validity of Benjamin's balances in the context of the lock-exchange flow of homogeneous fluids. By imposing energy conservation on the simplified time-dependent flow about the lock, Shin *et al.* (2004) derived a $Fr(a)$ formula which produces better agreement of the SW results with experiments than $Fr_B(a)$. In this case, the thickness of the current is half the initial height in the lock, in contrast with Benjamin's result that non-dissipative flows occur at $a = 0.5$ only. Shin *et al.* (2004) attribute this difference to energy transport by waves on the interface, which is omitted in Benjamin's balances. These results are expected to give rise to a controversy. In any case, the difficulty of verifying Benjamin's result by the lock-release experiments is evident even for the homogeneous ambient.

For the stratified-ambient case, the only relevant experimental study is also of the lock-release type. Maxworthy *et al.* (2002, hereinafter referred to as MLSM), investigated bottom gravity currents released from rectangular locks into linearly stratified ambients. The parameters H, S, g', and the lock geometry are known. The velocity of propagation, U, was accurately documented, but the corresponding values of h were not recorded. Consequently, a reliable reduction of the measured data to the form $U/(g'h)^{1/2}$ and $a = h/H$, which allows direct comparison with the theoretical $Fr(a, S)$, is not feasible. Moreover, the lock-release process generates internal gravity waves which may be incompatible with the assumptions of the theory. The interaction of the current with these waves in the subcritical regime tends to suppress the constant-velocity phase of propagation, as pointed out by Maxworthy *et al.* (2002). Nevertheless, a comparison was attempted to confirm the trends predicted by the theory, as follows.

To be specific, MLSM considered the release of a rectangular volume of dense fluid of height h_0 into a linearly stratified ambient of height H. The height ratios $a_0 = h_0/H = 1/3, 1/2, 2/3$ and 1, and various stratifications in the range $0.3 < S < 1$, were investigated. The experiments used salt water, clearly within the Boussinesq regime, and the typical Reynolds number was 10^4. In all cases, a phase of propagation with constant velocity was observed. This quasi steady-state 'slumping' phase resembles the steady-state assumption of the theoretical analysis. The corresponding velocity, U, obtained in laboratory experiments, was also confirmed by numerical simulations. The study expressed the velocity in the reduced form

$$\varphi = \frac{U}{\mathcal{N}H}. \tag{3.17}$$

(This dimensionless quantity is referred to as the Froude number Fr in MLSM, but we use a different notation to avoid confusion with our *Fr*.) An accurate summary of the results was represented by the fitted curves (see figure 7 of MLSM)

$$\varphi(R, a_0) = A(a_0) + C(a_0)\log R, \tag{3.18}$$

where $R = 1/S$, $a_0 = h_0/H$. The coefficients for the values $a_0 = \{1, 3/2, 1/2, 1/3\}$ are given by $A = \{0.266, 0.229, 0.205, 0.147\}$, and $C = \{0.912, 0.916, 0.846, 0.774\}$. As noted by MLSM, the current is supercritical when $\varphi > 1/\pi$, see (3.4).

The height of the nose of the current during the slumping stage is $h = \kappa h_0$, where κ is expected to be about $0.3 - 0.5$. The velocity of propagation, in terms of our analysis, is $U = Fr \times (g'\kappa h_0)^{1/2}$, with Fr calculated for $a = \kappa a_0$ and the appropriate S.

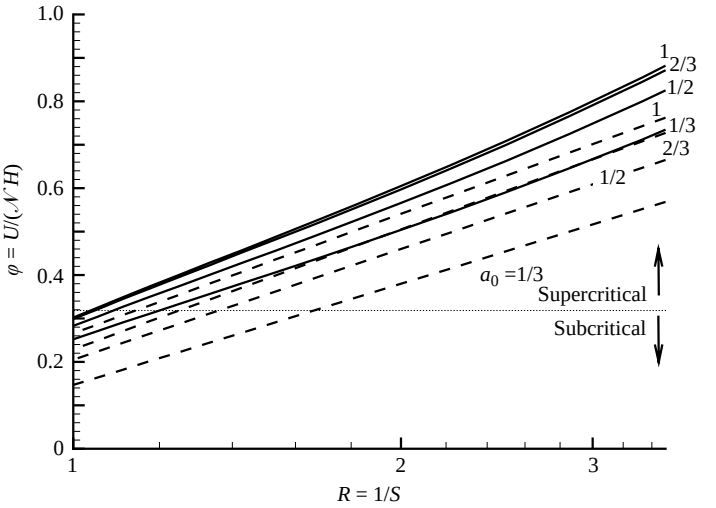

FIGURE 8. $U/(\mathcal{N}H)$ of a gravity current released from a lock of height h_0, as a function of $R = 1/S$ for various initial fractional depths $a_0 = h_0/H$. The dotted lines reproduce the experimental and numerical results of Maxworthy *et al.* (2002). The solid lines show the present theoretical approximation with $\kappa = 0.4$.

Substituting into (3.17), we can express the theoretical dependency as

$$\varphi = \kappa^{1/2} Fr(\kappa a_0, S) \frac{(g' h_0)^{1/2}}{\mathcal{N}H} = \kappa^{1/2} Fr(\kappa a_0, S) \left(\frac{h_0}{SH} \right)^{1/2}. \tag{3.19}$$

Using the present approximation (3.1) for $Fr(a, S)$ (practically valid for $S < 1$ in the present range of a) and rearranging, we obtain

$$\varphi = \left\{ \kappa^{1/2} Fr_B(\kappa a_0) \right\} \left[\left(\frac{h_0}{2H} \right) \left(2R - \tfrac{4}{3} \right) \right]^{1/2}, \tag{3.20}$$

where, again, $R = 1/S$, represents the stratification. The form of this result is similar with the experimental-heuristic inference of MLSM, equation (4), for large R (small S). The small formal difference is that the formula of MLSM contains 1 instead of 4/3 in the last term. MLSM denoted the term in the curly brackets by k, and pointed out that it is expected to depend on a_0. The good agreement between these formulae provides support to the present theory.

Unfortunately, the values of κ for the data set (3.18) are not available, and this prevents a sharp comparison of the reported real φ with the predictions of the present theory. To proceed, we introduce the plausible assumption $\kappa = 0.4$. An inspection of the flow-field figures presented in MLSM, and order-of-magnitude considerations, indicate that this is a fairly representative value (although the deviations about it may be large, in the range of 50 %). The comparison of the experimental–numerical data with the theoretical estimates (3.20) is displayed in figure 8; note that R is on a logarithmic axis, like in the corresponding figure 7 of MLSM. The real and theoretical results are consistent. In both experiment and theory, φ increases with R (almost linearly with respect to the log R axis), and with the depth ratio $a_0 = h_0/H$. The tendency for the current to be supercritical for large R (small S) and subcritical for small R (non-small S) is also well reproduced. As expected, for a given geometry and stratification, the theoretical inviscid speed of propagation is always larger

(by typically 30 %) than the measured values. This feature is well known for the unstratified cases, and it is seen here that it carries over to the stratified configuration.

A more accurate comparison between the theory and the real data requires knowledge of κ, i.e. the real height of the gravity current during the slumping phase. This topic is left for future work. When this information becomes available, the comparisons with the present theory can be performed easily along the lines shown here.

Another verification which is expected to throw light on the theory is the comparison of the present Fr results to previously suggested formulae for which some support has been gained. Ungarish & Huppert (2002) argued that

$$Fr(a, S) = Fr(a, S = 0)\left(1 - S + \tfrac{1}{2}aS\right)^{1/2}, \tag{3.21}$$

and, in the present context, $Fr(a, S=0) = Fr_B(a)$. Kao (1976) developed an ad hoc approximation for a deep intrusion with $S=1$; in the present notation it reads $Fr = a^{1/2}$. This result is a particular case of (3.21) (recall that $Fr_B \approx \sqrt{2}$ for small a) (Manins (1976) suggested, for $S=1$, a global volume-average Froude. This is incompatible with the present analysis). These suggestions were made in the framework of time-dependent propagation SW models for lock-release problems, and turn out to be related to the effective driving discussed in § 3.3. Kao (1976) performed comparisons with experi ments of Wu (1969). Ungarish & Huppert (2002, 2004) made detailed compari sons of the SW results with experimental and Navier–Stokes numerical data of Maxworthy *et al.* (2002), and with additional numerical simulations. Ungarish (2005) developed the corresponding SW theory for a symmetric intrusion and performed detailed comparisons with experiments of Wu (1969), Amen & Maxworthy (1980), Faust & Plate (1984) and Rooij (1999). Judging from the overall good agreement of the velocity of propagation, (3.21) captures fairly well the influence of a and S on the velocity. We therefore think that the comparison of (3.21) with the present more rigorous results may throw some light on the problem.

We denote by G the ratio between the present Fr to the suggested Ungarish–Huppert (HU) formula (3.21). This ratio depends on S, a, and on the number of the root (when the solution of (2.12) is not unique). The typical behaviour is shown in figure 9. For small S/a, the agreement is very good. In particular, for $S \leqslant 0.5$ and $a \geqslant 0.1$ the discrepancy is at most 16 %. On the other hand, for $S=0.8$ the first root solution exceeds the UH prediction by about 25 % at $a=0.3$ and by 65 % at $a=0.10$. However, the second and third roots display a better agreement, in the range of ± 20 % for $0.02 \leqslant a \leqslant 0.12$.

Additional information on the case $S=0.98$ is presented in figure 10. (We use this value as representative of the strongest stratification; for S closer to 1 some $\theta > 1$, difficulties appear in some circumstances.) For $S=0.98$ and small a, many valid roots are obtained: e.g. 6 and 13 for $a=0.05$ and 0.02, respectively. The results of the first roots exceed very significantly the HU formula, but for larger i (and γ_i) a fairly good agreement appears. The value of the invalidity-instability coefficient θ first decreases with the number of the root, and then increases. In the region of minimum θ (which we think is the most stable) the values of G are about 1.3. We therefore suggest the following criterion: when several solutions Fr are possible for given (a, S), the one with the smallest θ is expected to appear in practical cases.

From the point of view of application to real gravity currents, these findings are encouraging. The use of the UH formula in various circumstances produced, with no exception, simple predictions for the velocity of propagation which agree well

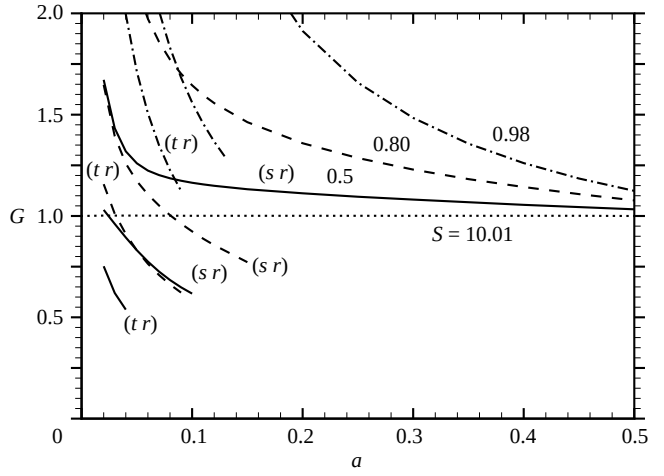

FIGURE 9. *Fr* ratio (present to UH formula), G, as a function of a for various S ($S = 0.01$ dotted line, $S = 0.5$ solid line, $S = 0.8$ dashed line, $S = 0.98$ dash-dotted line). The second and third root results are marked by (sr) and (tr), respectively.

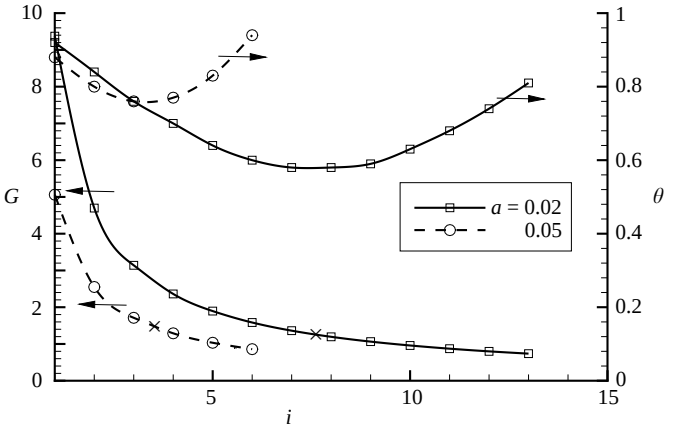

FIGURE 10. *Fr* ratio G and invalidity-instability coefficient θ as a function of root number i for $S = 0.98$, and two values of a: $a = 0.05$ dashed line, $a = 0.02$ solid line. The arrows indicate the axis for the line. The most plausible (minimum θ) results are marked by $\times$.

with available experimental and numerical results. The fact that the present theory endorses this formula for a very significant range of S and a provides support to the shallow-water modelling used by Ungarish & Huppert (2002). Conversely, this consistency indicates that the present analysis is not just an academic exercise, but rather captures the physical behaviour of real systems. However, we keep in mind that the validity-stability criterion used in the present theory lacks a rigorous foundation, and therefore more work is required to further verify the apparent agreements.

The *Fr* formulae derivations of Ungarish & Huppert (2002) and Kao (1976) ignore the validity-stability, dissipation and non-uniqueness features of the gravity current flow–field. These difficulties become important, theoretically, for $S > 0.5$. However, in practical release from behind a lock, the velocity develops from zero and hence it is plausible that the flow adjusts to the smallest (or close to it) possible velocity

of propagation. This corresponds to the subcritical branch and the larger γ_i roots. Therefore, no serious deviations from the over-simplified behaviour predicted by (3.21) were noted in lock-release experiments. On the other hand, we must keep in mind that the available experimental data cover a narrow domain of a, and are prone to wave contamination owing to the initial gate-removal motion. Indeed, Maxworthy *et al.* (2002) inferred from their experimental observations that for small a the initial flow in a lock-release experiment will be subcritical and will rapidly evolve into a time-dependent wavy state (see also Manasseh, Ching & Fernando 1998), with no measurable quasi-steady velocity of propagation. Moreover, the available experiments were performed in configurations with open surfaces. Another important point is the control of the possible influence of upstream waves on the validity of Long's unperturbed far-field assumption. It is therefore clear that the verification of the intriguing features of validity-stability, dissipation and non-uniqueness, pointed out by the present analysis in particular for small values of a, require special experiments. It is plausible that the initial/boundary conditions play an important role in establishing the multiple-solution regimes indicated by the present theory.

4. Concluding remarks

The classical *Fr* and dissipation results developed for a steady propagation of a gravity current by Benjamin (1968) have been generalized to a linearly stratified ambient. Like Benjamin's results, the evident significance of this progress is more in the fundamental-theoretical domain than in the practical consequences, at least at the present stage of knowledge. The theory provides support and guidelines for the investigation of real gravity currents, but cannot be used directly as a prediction tool. The steady-state flow assumption, irrespective of the initial conditions, restricts the applicability of the theoretical *Fr* and dissipation formulae to the head region of a practical current, and even this only as a first approximation.

The study proves three main points. (i) For weak stratifications and not very deep ambients (say, $S < 0.5$ and $a > 0.1$), the stratification causes a simple decrease of the speed of propagation and dissipation as compared with the non-stratified results for the same fractional depth, a. In this case, the current is supercritical and unique (for given a and S). (ii) For larger S and/or small a, the situation is complicated by the existence of several apparently acceptable results for a given combination of S and a. The current may be subcritical. A plausible criterion for the selection of the physically expected results was suggested (the theoretical or physical foundation of this criterion is still lacking). (iii) No steady-state currents are possible for $a > a_{max}(S)$, where $a_{max}(S)$ is 0.5 in the non-stratified limit and decreases with S. (To be specific, we have in mind a system in which the density of the current, ρ_c, and at the top of the ambient ρ_o ($< \rho_c$) , are fixed. The density in the ambient increases linearly to a prescribed value at the bottom, ρ_b ($\leqslant \rho_c$). The strength of stratification, S, specifies, on a scale from 0 to 1, the position of ρ_b between ρ_o to ρ_c. The geometry is expressed by the height ratio of the current to ambient, a. The criticality is with respect to the fastest internal gravity wave mode in the unperturbed ambient.)

The dissipation of the system decreases with S. In the higher-roots results, the head loss (scaled with h) is very small. In these cases, the difference from energy conserving solutions is expected to be negligible. The development of an energy conserving counterpart theory is left for future work.

The assumptions necessary for obtaining the solution of this formidable problem, and in particular the use of Long's model, are compatible with these underlying

Benjamin's flow field. This is reflected by the full agreement between the results when $S \to 0$. The hydrostatic simplification in Long's model means that the typical vertical displacement of the streamline, δ, occurs over a relatively much larger horizontal distance. The use of the inviscid global flow-force balance may be justified when $Re = Uh/\nu \gg 1$. These restrictions are mild, and consistent with the inviscid shallow-water modelling, which is the widely accepted tool in the investigation of gravity currents. The Boussinesq assumption can, formally, be relaxed – but, judging from the complexity of the present analysis, there is little hope of obtaining meaningful non-Boussinesq analytical results. This topic is left for future work. The assumption of an unperturbed upstream domain is, perhaps, the weakest point of Long's model when the current is subcritical. A guideline is provided by experiments with flows over a rigid topography in geometries which resemble a gravity current (Baines 1995, § 5.6). For conditions relevant to the present supercritical flows, no disturbances were observed on the upstream side. On the other hand, for the subcritical counterpart, perturbations corresponding to columnar modes were sometimes observed on the upstream side. These persistent upstream perturbations are an indication that the simple upstream boundary conditions are sometimes incompatible with the existence of an obstacle in the fluid. Nevertheless, Long's model (and the present solution) are expected to be a good approximation if the amplitude of these perturbations is small. Since a gravity current is a flexible obstacle and the validity-stability conditions are imposed by our analysis, we can speculate that upstream perturbations (if any) will be milder in our case than in the experiments discussed by Baines (1995). Indeed, there are some experimental indications that these upstream perturbations are very weak in flows of intrusions (Rooij 1999). The practical effect of this difficulty, and the related issue of multiple solutions, require further, mostly experimental, investigation. We think that the present theory provides both the motivation and the required guidelines for these experiments.

REFERENCES

Amen, R. & Maxworthy, T. 1980 The gravitational collapse of a mixed region into a linearly stratified fluid. *J. Fluid Mech.* **96**, 65–80.

Baines, P. G. 1995 *Topographic Effects in Stratified Flows.* Cambridge University Press.

Benjamin, T. B. 1968 Gravity currents and related phenomena. *J. Fluid Mech.* **31**, 209–248.

Faust, K. M. & Plate, E. J. 1984 Experimental investigation of intrusive gravity currents entering stably stratified fluids. *J. Hydraul. Res.* **22**, 315–325.

Härtel, C., Meiburg, E. & Necker, F. 2000 Analysis and direct numerical simulation of the flow at a gravity current head. Part 1. Flow topology and front speed. *J. Fluid Mech.* **418**, 189–212.

Huppert, H. E. & Simpson, J. E. 1980 The slumping of gravity currents. *J. Fluid Mech.* **99**, 785–799.

Kao, T. W. 1976 Principal stage of wake collapse in a stratified fluid: two-dimensional theory. *Phys. Fluids* **19**, 1071–1074.

Klemp, J. B., Rotunno, R. & Skamarock, W. C. 1994 On the dynamics of gravity currents in a channel. *J. Fluid Mech.* **269**, 169–198.

Long, R. R. 1953 Some aspects of the flow of stratified fluids. I. A theoretical investigation. *Tellus* **5**, 42–58.

Long, R. R. 1955 Some aspects of the flow of stratified fluids. III. Continuous density gradients. *Tellus* **7**, 341–357.

Manasseh, R., Ching, C.-Y. & Fernando, H. J. S. 1998 The transition from density-driven to wave-dominated isolated flows. *J. Fluid Mech.* **361**, 253–274.

Manins, P. C. 1976 Mixed region collapse in a stratified fluid. *J. Fluid Mech.* **77**, 177–183.

Maxworthy, T., Leilich, J., Simpson, J. E. & Meiburg, E. H. 2002 The propagation of gravity currents in a linearly stratified fluid. *J. Fluid Mech.* **453**, 371–394 (referred to as MLSM).

DE ROOIJ, F. 1999 Sedimenting particle-laden flows in confined geometries. PhD thesis, DAMTP, University of Cambridge.

SHIN, J. O., DALZIEL, S. B. & LINDEN, P. F. 2004 Gravity currents produced by lock exchange. *J. Fluid Mech.* **521**, 1–34.

SIMPSON, J. & BRITTER, R. E. 1979 The dynamics of the head of a gravity current advancing over a horizontal surface. *J. Fluid Mech.* **94**, 477–495.

UNGARISH, M. 2005 Intrusive gravity currents in a stratified ambient: shallow-water theory and numerical results. *J. Fluid Mech.* **535**, 287–323.

UNGARISH, M. & HUPPERT, H. 2002 On gravity currents propagating at the base of a stratified ambient. *J. Fluid Mech.* **458**, 283–301.

UNGARISH, M. & HUPPERT, H. 2004 On gravity currents propagating at the base of a stratified ambient: effects of geometrical constraints and rotation. *J. Fluid Mech.* **521**, 69–104.

WU, J. 1969 Mixed region collapse with internal wave generation in a density-stratified medium. *J. Fluid Mech.* **35**, 531–544.